

Influence of Size Effect on the Electronic and Elastic Properties of Diamond Films with Nanometer Thickness

Leonid A. Chernozatonskii,^{*,†} Pavel B. Sorokin,^{‡,§} Alexander A. Kuzubov,[‡] Boris P. Sorokin,[#] Alexander G. Kvashnin,^{‡,¶} Dmitry G. Kvashnin,[‡] Pavel V. Avramov,^{‡,||} and Boris I. Yakobson[§]

Emanuel Institute of Biochemical Physics, Russian Academy of Sciences, 4 Kosigina Street, Moscow, 119334, Russian Federation, Siberian Federal University, 79 Svobodny Avenue, Krasnoyarsk, 660041 Russian Federation, Department of Mechanical Engineering & Material Science and Department of Chemistry, Rice University, Houston, Texas 77251, United States, Technological Institute of Superhard and Novel Carbon Materials, 7a Centralnaya Street, Troitsk, Moscow Region, 142190, Russia, Kirensky Institute of Physics, Russian Academy of Sciences, Akademgorodok, Krasnoyarsk, 660036 Russian Federation, and Advanced Science Research Center, Japan Atomic Energy Agency, Tokai, Ibaraki319-1195, Japan

Received: August 25, 2010; Revised Manuscript Received: October 19, 2010

The atomic structure and physical properties of few-layered $\langle 111 \rangle$ oriented diamond nanocrystals (diamanes), covered by hydrogen atoms from both sides, are studied using electronic band structure calculations. It was shown that energy stability linearly increases upon increasing of the thickness of proposed structures. All 2D carbon films display direct dielectric band gaps with nonlinear quantum confinement response upon the thickness. Elastic properties of diamanes reveal complex dependence upon increasing of the number of $\langle 111 \rangle$ layers. All theoretical results were compared with available experimental data.

Introduction

Graphene as a two-dimensional material has attracted attention from the scientific community long before experimental fabrication. The first theoretical study of graphene dates to 1946, when the remarkable band structure of “Dirac cones” was studied.¹ The first experimental observation of free-standing graphene² in 2004 initiated the comprehensive study of this material. Ballistic conductivity, pseudo-chiral Dirac’s nature of carriers, and anomalous Hall effect³ make graphene the most promising material for science and future technology.

Hydrogenation of graphene enlarges its potential application in nanoelectronics. Regular adsorption of hydrogen atoms changes graphene’s electronic structure and opens the band gap depending upon the distance between hydrogen regions.^{4–8} Total hydrogenation of graphene changes the nature of electronic states due to changing of sp^2 hybridization of C–C bonds to a sp^3 one and opens the dielectric band gap.^{9,10} Such a two-dimensional insulator was called graphane.¹⁰ The theoretical prediction was generally confirmed experimentally by Elias et al.¹¹

Graphane is an offspring of graphene along with graphene nanoribbons and carbon nanotubes. The other type of carbon bonding opens a new way of developing two-dimensional carbon-based materials.

Graphane is the first member in a series of sp^3 -bonded diamond films consisting of a number of adjusted $\langle 111 \rangle$ oriented layers which display unique physical properties. For the first

time diamane structures were proposed by Chernozatonskii et al.¹² in 2009. Recently¹³ a similar C_2H structure was also considered.

Usually diamond films are prepared by the CVD method with micrometer thickness.¹⁴ Also, the diamond quantum wells are obtained in the bulk structures of superlattices.¹⁵ The consequent study of graphene, graphane, and proposed diamanes can be considered as a bottom-up nanotechnological approach opposite to an ordinary top-down paradigm. The main goal of this work is to study diamane physical properties. Unlike ref 12, we consider diamanes with different thicknesses and investigate their stability and compare them with known data for sp^3 -hybridized hydrocarbon clusters. We study the elastic properties of the structures and obtain phonon dispersion, wave velocities, and elastic constants. Finally, we discuss possible ways to synthesize the structures.

Method and Model

The plane-wave DFT PBE¹⁶ electronic structure calculations of 2D carbon nanostructures were performed using ultrasoft Vanderbilt pseudopotentials¹⁷ and a plane-wave energy cutoff equal to 30 Ry by PWSCF code.¹⁸ To calculate equilibrium atomic structures, the Brillouin zone was sampled according to the Monkhorst–Pack¹⁹ scheme with a $16 \times 16 \times 1$ k-point convergence grid. To avoid interactions between the species, neighboring planes were separated at least by 10 Å in the hexagonal supercells. During the atomic structure minimization, structural relaxation was performed until the change in total energy was less than 3×10^{-7} eV. Phonons calculations were performed within density functional perturbation theory.²⁰ All the values given above were carefully tested and found optimal.

Results and Discussion

Atomic structures of graphene and graphane are presented in Figure 1a and b, respectively. Both structures display

* To whom correspondence should be addressed. E-mail: cherno@sky.chph.ras.ru.

[†] Emanuel Institute of Biochemical Physics, Russian Academy of Sciences.

[‡] Siberian Federal University.

[§] Rice University.

[#] Technological Institute of Superhard and Novel Carbon Materials.

[¶] Kirensky Institute of Physics, Russian Academy of Sciences.

^{||} Japan Atomic Energy Agency.

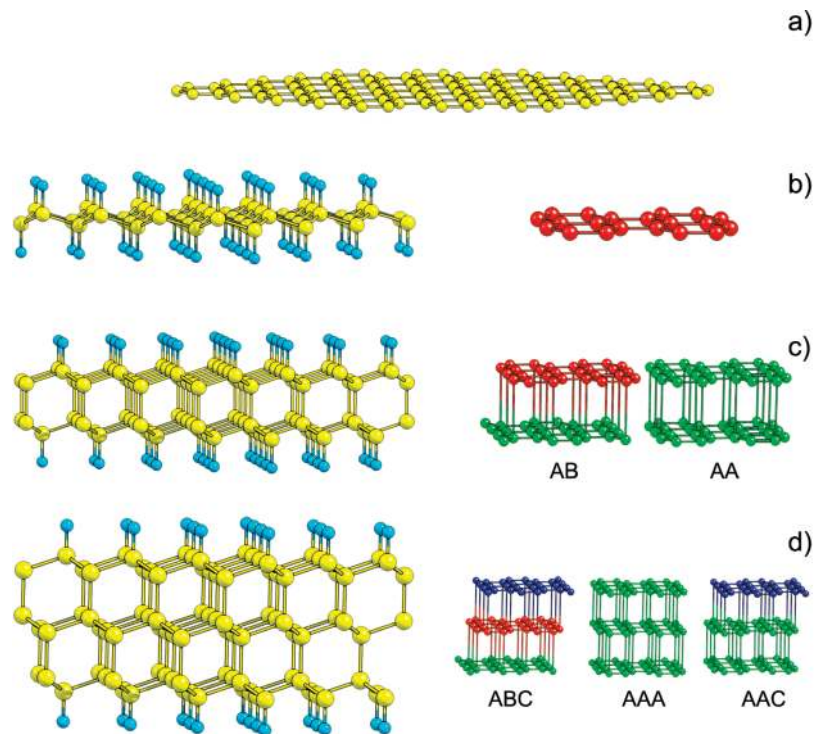


Figure 1. Atomic geometry of studied quasi two-dimensional carbon nanofilms: (a) graphene; (b) graphane; (c) diamane D(AB) with AB stacking of two layers; (d) diamane D(ABC) with ABC stacking of three layers. Carbon atoms are marked by yellow (light gray); hydrogen atoms are marked by blue (gray). For each diamane, possible stacking sequences of carbon layers are presented.

hexagonal symmetry with essentially different lattice parameters (2.468 and 2.540 Å, respectively) because of different nature of chemical bonding. In contrast to flat sp^2 -hybridized graphene, crimped sp^3 graphane is characterized by two terminal layers of hydrogen atoms from both sides of the sheet. Surface hydrogen atoms of graphane at least from one side can be replaced by one more layer of sp^3 carbon atoms forming a diamane structure. Since chemical bonding between carbon layers in diamanes is also realized by sp^3 hybridization, the lattice parameters of studied diamanes are close to each other ($a = 2.53$ Å).

Hydration of graphene completely changes the nature of the material which can be considered as the thinnest possible diamond. The diamond films with smallest thickness obviously succeed the properties of the graphane with consistent approaching of the bulk diamond limit. Diamond films or diamanes under study fill the gap between two-dimensional graphane and crystalline diamond.

The atomic geometry of the diamane consists of stacking covalently bounded monatomic carbon layers (Figure 1c,d). The changing of the stacking sequence allows constructing different diamane polytypes. According to this fact, diamanes can be compactly classified as $D(ijk...l)$ where i, j, k, l are positions layer types which can be equal to A, B, or C. For example, two- and three-layered diamanes with natural diamond stacking sequence (ABCABC...) are denoted as D(AB) and D(ABC); two- and three-layered diamanes with lonsdaleite stacking sequence (AAA...) are denoted as D(AA) and D(AAA). In the left part of Figure 1c–d, the D(AB) and D(ABC) structures are presented, whereas on the right possible stacking sequences of carbon layers in corresponding diamanes are shown. In general, graphane can be named as D(A), but we suppose that graphane is the intermediate structure between graphane and diamane due to the fact that the structure does not contain any diamond-like cells.

Formation energy (eV/atom) of studied structures was calculated according to the following equation:^{21,22} $E_{\text{form}} = (E_{\text{str}} - nE_{\text{graphene}} - 2E_{\text{H}_2})/(n + 2)$, where E_{graphene} is the energy of graphene per carbon atom (−9.30 eV/atom), E_{H_2} is the energy of the hydrogen molecule (−2.99 eV/atom), and n is the number of carbon atoms in the unit cell.

For the sake of comparison, the formation energies of a set of hydrocarbon structures were calculated using the same PBC DFT method. Studied structures can be divided into three groups. The first group (molecules) contains one member, CH_4 molecule which has the lowest formation energy (−0.25 eV/atom). The next group consists of diamondoids and contains three smallest members of the family: adamantane, diamantine, and triamantane.²³ The third group (two-dimensional diamond-like nanothick films) contains graphane and diamanes.

The energies of the studied structures tend to be nearly linear to the energy of bulk diamond (Figure 2a) upon the hydrogen content. The diamanes with diamond type layer stacking (AB and ABC types) display the lowest energy per atom in comparison with corresponding structures with other stacking sequences, but the difference in the energy of diamanes with diamond and other stacking sequences is smaller than 0.02 eV/atom which justifies the possible existence of diamanes with any stacking types. Two-layered diamanes $D(ij)$ are less favorable than graphane but are more favorable than graphene. The stability of the $D(ij)$ is also proved by the high energy of 0.74 eV/atom of separation of D(AB) to two isolated carbon layers hydrogenated from one side.

Figure 2a allows to estimate a possible way to prepare diamanes. The formation energy of three-layered diamanes is positive (in the assumption of zero temperature and pressure) if graphane and H_2 are used as source species of carbon and hydrogen atoms, respectively. The changing of the source of hydrogen from molecular H_2 to atomic H leads to a different sign of the formation energy from positive to negative which

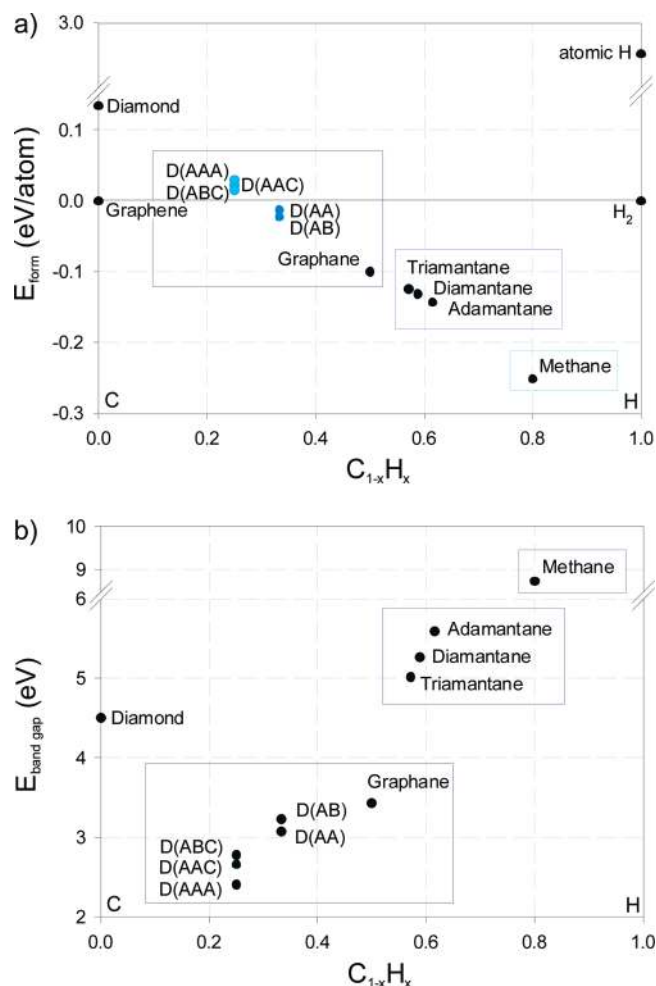


Figure 2. (a) Formation energy and (b) band gap width of different hydrocarbon structures as a function of hydrogen content. One can see three groups of structures marked by rectangles. The first group consists of sp^3 -hybridized CH_4 molecule. The next group consists of several members of diamondoid family (adamantane, diamantine, and triamantane²³). The last group consists of 2D nanoclusters of graphane and diamanes $D(ij)$ and $D(ijk)$.

means that all studied diamane series become energy favorable. It should be noted that the graphane-like structure was synthesized experimentally using by atomic hydrogen.¹¹ In the case of diamanes, passivating hydrogen layers display only hexagonal symmetry in contrast to graphane on which surface hydrogen can be arranged in various manners.^{9,10,24}

Let us consider the electronic properties of the studied structures. Band structures of graphane and diamanes are similar and display dielectric behavior and direct band gap. For the sake of comparison, the electronic structure of methane and diamondoid clusters was also calculated. The band gap of studied structures should tend to the band gap of bulk diamond (Figure 2b) upon the decrease of hydrogen content (and increase of the thickness of the structure). In the case of diamondoid clusters, similar results were obtained in ref 25. The diamane band gap widths are lower than the gap of graphane (3.4 eV) which is evidence of the existence of a minimum in the dependence of band gap value upon the number of layers because the calculated band gap of diamond (diamane with infinite index) is 4.5 eV. The nonlinear effect of the studied films can be explained by surface states and quantum confinement effect. During the increasing of diamane film thickness, the contribution of electrons from the bulk increases and electronic properties of the diamanes tend to the properties of diamond.

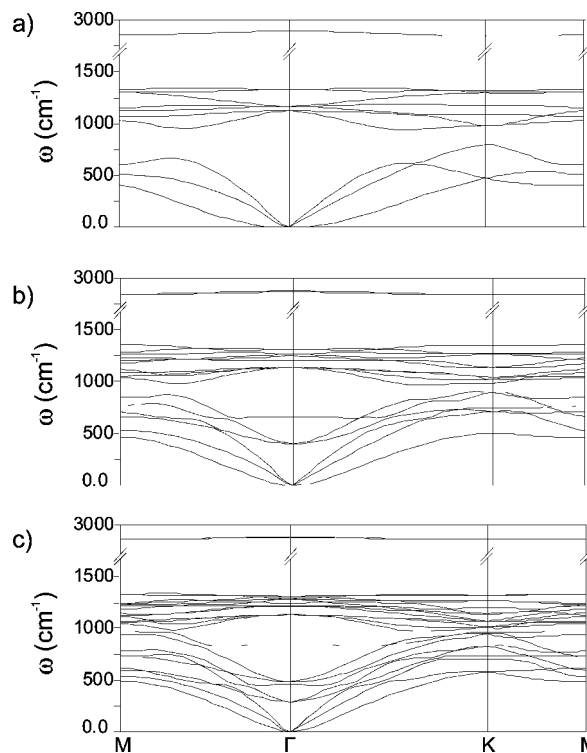


Figure 3. Phonon band structures of 2D carbon nanostructures: (a) graphane; (b) D(AB); (c) D(ABC).

The phonon band structures of graphane, D(AB) and D(ABC), are presented in Figure 3 (a, b and c, respectively). The energy splitting of the graphane highest active modes in Raman spectrum (2856 and 2896 cm^{-1} , reference values¹⁰ are 2842 and 2919 cm^{-1}) is equal to 40 cm^{-1} , whereas diamanes display smaller energy splitting of the modes (2865 and 2875 cm^{-1} for D(AB), and 2874 and 2882 cm^{-1} for D(ABC), respectively); see group VI in Table 1. The increasing of the number of modes in the frequency region around 1332 cm^{-1} (diamond fingerprints) can be an indication of diamane films due to linear increase of line intensities upon thickness of the diamond-like film²⁶ (group V in Table 1). Another characteristic feature of diamanes is appearance of the vibrational modes at 664 and 848 cm^{-1} in the cases of D(AB) and D(ABC), respectively (group III in Table 1). Near the 500 cm^{-1} frequency region one can see two (for D(AB)) and five (for D(ABC)) optical modes bunched in one and two groups, respectively (groups I and II in Table 1).

Three acoustic branches of graphane and diamanes correspond to in-plane (two branches, linear dependence $\omega(k)$) and out-plane (one branch, quadratic dependence $\omega(k)$) vibrations of the 2D structure.²⁷ The increasing of the thickness of the film leads to gradual transformation of the quadratic branch to a linear one of transverse mode typical for the crystal.

Velocities of longitudinal and transverse acoustic in-plane modes (Table 1) were obtained from phonon spectra (Figure 3). For comparison the longitudinal and transverse velocities were calculated for diamond in hexagonal orientation based on the experimental value of elastic constants²⁸ (see Supporting Information for details). It is clearly seen that the velocities are gradually increased with increasing of the thickness of the films due to the augmentation of stiffness of the structures and tend to the diamond values.

Based on the velocities, elastic constants of graphane, graphane, D(AB), and D(ABC) were calculated and compared with experimental data for graphite²⁹ and theoretical data for

TABLE 1: Phonon Frequencies (cm^{-1}) at the Γ -Point Region and Velocities of Transverse and Longitudinal Acoustic in-Plane Modes (10^3 m/s)

I	ω_{opt} groups								v_{TA}	v_{LA}
	II	III	IV	V	VI					
graphane	–	–	–	1123, 1123	1159, 1162, 1162, 1328, 1328	1159, 1162, 1162, 1328, 1328	2856, 2896	12.0	17.7	
D(AB)	401, 401		664	1131, 1131, 1133, 1133	1201, 1249, 1260, 1260, 1313, 1313	1201, 1249, 1260, 1260, 1313, 1313	2865, 2875	12.1	17.8	
D(ABC)	291, 291	467, 483, 483	848	1132, 1132, 1133, 1133	1211, 1224, 1224, 1248, 1282, 1287, 1287, 1308, 1308	1211, 1224, 1224, 1248, 1282, 1287, 1287, 1308, 1308	2874 2882	12.2	18.0	
diamond (experiment ²⁸)								12.4	18.3	

TABLE 2: Density ρ_{2D} , Elastic Constants C_{11} and C_{12} , and Poisson's Ratio σ of 2D Nanostructures

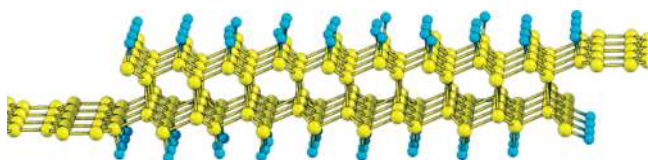
	ρ_{2D} (10^{-7} kg/m ²)	C_{11} (N/m)	C_{12} (N/m)	σ
graphene	7.55	349, 358.1, ³⁰ 308.2, ³¹ 355.1 \pm 20.1 ²⁹	61.5, 60.4, ³⁰ 80.4, ³¹ 60.3 \pm 6.7 ²⁹	0.176, 0.167, ³⁰ 0.261, ³¹ 0.16, ³² 0.17 \pm 0.01 ²⁹
graphane	7.73	242, 243, ³² 245 ³³	19.5	0.081, 0.07 ³²
D(AB)	14.9	474	35.9	0.076
D(ABC)	22.2	718	58.3	0.081

graphene^{30,31} and graphane.³² Due to the 2D nature of the objects under study, the elastic constants were calculated using the equations $C_{11} = v_{\text{TA}}^2 \rho_{2D}$ and $C_{12} = C_{11} - 2v_{\text{TA}}^2 \rho_{2D}$, where ρ_{2D} is formal density (kg/m² units) in which ambiguous thickness of 2D material is neglected. To compare the calculated data and experimental values of elastic constants of bulk graphite from ref 29, the theoretical data of graphene from ref 31 were multiplied by the formal value 3.35 Å (the distance between graphene layers in graphite).

Graphane displays lower stiffness than graphene due to the sp^3 corrugation of graphane structure which allows higher elasticity.^{32,33} Two-layered diamane has a bigger expected C_{11} constant than graphene but smaller C_{12} which leads to smaller Poisson's coefficient (Table 2). The same result was obtained for graphane in the work of ref 32. In diamanes the surface and bulk carbon atoms make practically the same contribution to the stiffness of the film due to the absence of surface reconstruction.

Finally, we discuss the possible methods of diamane fabrication. The adsorption of hydrogen atoms on the outer layers of multilayered graphene transforms the sp^2 carbon bonds to sp^3 ones. Such layers display a deficiency of electrons and can connect with inner layers of the structure and form diamond cells and eventually diamane film.

Previously¹³ it was shown that during the formation of bonds between bigraphene layers with adsorbed hydrogen atoms the formation energy goes down, demonstrating a possibility of diamane synthesis. One more possibility to synthesize diamanes is an overlapping of the ends of graphene ribbons or graphenes (Figure 4). The Brenner empirical potential³⁴ was used for the relaxation and calculation of energy stability of two overlapped ribbons. It was obtained that such a structure is stable and energetically favorable.

**Figure 4.** Relaxed structure of two graphene ribbons with a diamane region between them.

Hydrogenated graphene layers were studied in the paper of Luo et al.,³⁵ and Raman spectra of hydrogenated single, double, triple, etc., graphene were obtained. The increasing of the intensity of the D band in the vicinity of the 1340 cm^{-1} region with increasing of the number of graphene layers can be associated with appearance of diamane parts in the structure. One more experimental evidence of diamane growth is a synthesis of diamond films with crystalline structure.³⁶

The electronic structure calculations directly demonstrate complex dependence of the physical properties of diamanes upon their thickness. Controllable variation of the number of $\langle 111 \rangle$ layers and sequence order leads to tunable variation of electronic properties of diamanes. Diamanes can be applied in nanoelectronics and nanooptics, e.g., as active laser medium within lasers. The increasing number of layers in diamane will lead to the transition of direct band gap to indirect one (diamond); therefore, only thin films can be used for this purpose. Diamanes can be used as optical planar waveguides and as very thin dielectric hard films in nanocapacitors or as chemical nanosensors (e.g., it was obtained that hydrogenated diamond surfaces change their electrical conductivity by adsorption of H_3O^+ species³⁷) or as mechanically stiff nanothick elements in nanoelectronics.

Acknowledgment. L.A.C. was supported by the Russian Academy of Sciences, program No. 21 and by the Russian Foundation for Basic Research (project no. 08-02-01096). P.B.S. and B.I.Y. acknowledge support by the Office of Naval Research (MURI project). P.V.A. and P.B.S. also acknowledge the collaborative RFBR-JSPS grant no. 09-02-92107-ЯФ. We are grateful to the Joint Supercomputer Center of the Russian Academy of Sciences for the possibility of using a cluster computer for quantum chemical calculations. The geometry of all presented structures was visualized by commercial Chem-Craft software.

Supporting Information Available: Longitudinal and transverse velocities calculated for diamond in hexagonal orientation based on the experimental value of elastic constants. This material is available free of charge via the Internet at <http://pubs.acs.org>.

References and Notes

- (1) Wallace, P. R. The band theory of graphite. *Phys. Rev. B* **1946**, *71*, 622–634.
- (2) Novoselov, K. S.; Jiang, D.; Schedin, F.; Booth, T. J.; Khotkevich, V. V.; Morozov, S. V.; Geim, A. K. Two-dimensional atomic crystals. *Proc. Natl. Acad. Sci. U.S.A.* **2005**, *102*, 10451–10453.
- (3) Neto, A. H. C.; Guinea, F.; Peres, N. M. R.; Novoselov, K. S.; Geim, A. K. The electronic properties of graphene. *Rev. Mod. Phys.* **2009**, *81*, 109.
- (4) Duplock, E. J.; Scheffler, M.; Lindan, P. J. D. Hallmark of perfect graphene. *Phys. Rev. Lett.* **2004**, *92*, 225502.
- (5) Chernozatonskii, L. A.; Sorokin, P. B. Nanoengineering structures on graphene with adsorbed hydrogen lines. *J. Phys. Chem. C* **2010**, *114*, 3225.
- (6) Chernozatonskii, L. A.; Sorokin, P. B.; Brüning, J. W. Two-dimensional semiconducting nanostructures based on single graphene sheets with lines of adsorbed hydrogen atoms. *Appl. Phys. Lett.* **2007**, *91*, 183103.
- (7) Singh, A. K.; Yakobson, B. I. Electronics and magnetism of patterned graphene nanoroads. *Nano Lett.* **2009**, *9*, 1540–1543.
- (8) Balog, R.; Jørgensen, B.; Nilsson, L.; Andersen, M.; Rienks, E.; Bianchi, M.; Fanetti, M.; Lægsgaard, E.; Baraldi, A.; Lizzit, S.; Slijivancanin, Z.; Besenbacher, F.; Hammer, B.; Pedersen, T. G.; Hornekar, P. H. Bandgap opening in graphene induced by patterned hydrogen adsorption. *Nat. Mater.* **2010**, *9*, 315–319.
- (9) Sluiter, M. H. F.; Kawazoe, Y. Cluster expansion method for adsorption: Application to hydrogen chemisorption on graphene. *Phys. Rev. B* **2003**, *68*, 085410.
- (10) Sofo, J. O.; Chaudhari, A. S.; Barber, G. D. Graphane: A two-dimensional hydrocarbon. *Phys. Rev. B* **2007**, *75*, 153401.
- (11) Elias, D. C.; Nair, R. R.; Mohiuddin, T. M. G.; Morozov, S. V.; Blake, P.; Halsall, M. P.; Ferrari, A. C.; Boukhalov, D. W.; Katsnelson, M. I.; Geim, A. K. Control of graphene's properties by reversible hydrogenation: Evidence for graphane. *Science* **2009**, *323*, 610.
- (12) Chernozatonskii, L. A.; Sorokin, P. B.; Kvashnin, A. G.; Kvashnin, D. G. Diamond-like C 2 H nanolayer, diamane: Simulation of the structure and properties. *JETP Lett.* **2009**, *90*, 134–138.
- (13) Leenaerts, O.; Partoens, B.; Peeters, F. M. Hydrogenation of bilayer graphene and the formation of bilayer graphane from first principles. *Phys. Rev. B* **2009**, *80*, 245422.
- (14) Ashfold, M. N. R.; May, P. W.; Rego, C. A.; Everitt, N. M. Thin film diamond by chemical vapour deposition methods. *Chem. Soc. Rev.* **1994**, *23*, 21–30.
- (15) Silva, S. R. P.; Amaratunga, G. A. J.; Haq, S.; Salje, E. K. Optical quantum size effects in diamond-like carbon superlattice structures. *Thin Solid Films* **1994**, *253*, 20–24.
- (16) Perdew, J. P.; Burke, K.; Ernzerhof, M. Generalized gradient approximation made simple. *Phys. Rev. Lett.* **1996**, *77*, 3865–3868.
- (17) Vanderbilt, D. Soft self-consistent pseudopotentials in a generalized eigenvalue formalism. *Phys. Rev. B* **1990**, *41*, 7892–7895.
- (18) Giannozzi, P.; Baroni, S.; Bonini, N.; Calandra, M.; Car, R.; Cavazzoni, C.; Ceresoli, D.; Chiarotti, G. L.; Cococcioni, M.; Dabo, I.; Corso, A. D.; de Gironcoli, S.; Fabris, S.; Fratesi, G.; Gebauer, R.; Gerstmann, U.; Gougoussis, C.; Kokalj, A.; Lazzeri, M.; Martin-Samos, L.; Marzari, N.; Mauri, F.; Mazzarello, R.; Paolini, S.; Pasquarello, A.; Paulatto, L.; Sbraccia, C.; Scandolo, S.; Sclauzero, G.; Seitsonen, A. P.; Smogunov, A.; Umari, P.; Wentzcovitch, R. M. QUANTUM ESPRESSO: A modular and open-source software project for quantum simulations of materials. *J. Phys.: Condens. Matter* **2009**, *21*, 395502.
- (19) Monkhorst, H. J.; Pack, J. D. Special points for Brillouin-zone integrations. *Phys. Rev. B* **1976**, *13*, 5188–5192.
- (20) Baroni, S.; de Gironcoli, S.; Dal Corso, A.; Giannozzi, P. Phonons and related crystal properties from density-functional perturbation theory. *Rev. Mod. Phys.* **2001**, *73*, 515–562.
- (21) Dumitrica, T.; Hua, M.; Yakobson, B. I. Endohedral silicon nanotubes as thinnest silicide wires. *Phys. Rev. B* **2004**, *70*, 241303(R).
- (22) Sorokin, P. B.; Chernozatonskii, L. A.; Avramov, P. V.; Yakobson, B. I. Magnesium boride nanotubes: Relative stability and atomic and electronic structure. *J. Phys. Chem. C* **2010**, *114*, 4852–4856.
- (23) Dahl, J. E.; Liu, S. G.; Carlson, R. M. K. Isolation and structure of higher diamondoids, nanometer-sized diamond molecules. *Science* **2003**, *299*, 96–99.
- (24) Artyukhov, V. I.; Chernozatonskii, L. A. Structure and layer interaction in carbon monofluoride and graphane: A comparative computational study. *J. Phys. Chem. C* **2010**, *114*, 5389–5396.
- (25) Landt, L.; Klünder, K.; Dahl, J. E.; Carlson, R. M. K.; Möller, T.; Bostedt, C. Optical response of diamond nanocrystals as a function of particle size, shape, and symmetry. *Phys. Rev. Lett.* **2009**, *103*, 047402.
- (26) Knight, D. S.; White, W. B. Characterization of diamond films by Raman spectroscopy. *J. Mater. Res.* **1989**, *4*, 385–393.
- (27) Saito, R.; Dresselhaus, G.; Dresselhaus, M. S. *Physical Properties of Carbon Nanotubes*, 1st ed.; Imperial College Press: London, 1998; p 259.
- (28) McSkimin, H. J.; Andreatch, P. Elastic moduli of diamond as a function of pressure and temperature. *J. Appl. Phys.* **1972**, *43*, 2944.
- (29) Blakslée, O. L.; Proctor, D. G.; Seldin, E. J.; Spence, G. B.; Weng, T. Elastic constants of compression annealed pyrolytic graphite. *J. Appl. Phys.* **1970**, *41*, 3373.
- (30) Wei, X.; Fragneaud, B.; Marianetti, C. A.; Kysar, J. W. Nonlinear elastic behavior of graphane: Ab initio calculations to continuum description. *Phys. Rev. B* **2009**, *80*, 205407.
- (31) Falkovsky, L. Phonon dispersion in graphene. *JETP* **2007**, *105*, 397–403.
- (32) Topsakal, M.; Cahangirov, S.; Ciraci, S. Strain induced modifications on the properties of graphane. *Appl. Phys. Lett.* **2010**, *96*, 091912.
- (33) Muñoz, E.; Singh, A. K.; Ribas, M. A.; Penev, E. S.; Yakobson, B. I. The ultimate diamond slab: GraphAne versus graphEne. *Diamond Relat. Mater.* **2010**, *19*, 368–373.
- (34) Brenner, D. W.; Shenderova, O. A.; Harrison, J. A.; Stuart, S. J.; Ni, B.; Sinnott, S. B. A second-generation reactive empirical bond order (REBO) potential energy expression for hydrocarbons. *J. Phys.: Condens. Matter* **2002**, *14*, 783–802.
- (35) Luo, Z.; Yu, T.; Kim, K.; Ni, Z.; You, Y.; Lim, S.; Shen, Z.; Wang, S.; Lin, J. Thickness-dependent reversible hydrogenation of graphene layers. *ACS Nano* **2009**, *3*, 1781–1788.
- (36) Tsugawa, K.; Ishihara, M.; Kim, J.; Koga, Y.; Hasegawa, M. Nucleation enhancement of nanocrystalline diamond growth at low substrate temperatures by adamantane seeding. *J. Phys. Chem. C* **2010**, *114*, 3822–3824.
- (37) Andriotis, A. N.; Mpourmpakis, G.; Richter, E.; Menon, M. Surface conductivity of hydrogenated diamond films. *Phys. Rev. Lett.* **2008**, *100*, 106801.